IEEE Access
Multidisciplinary | Rapid Review | Open Access Journal

Received December 25, 2018, accepted January 16, 2019, date of publication January 24, 2019, date of current version February 14, 2019.

Digital Object Identifier 10.1109/ACCESS.2019.2894840

A New Frequency Control Strategy in an Islanded Microgrid Using Virtual Inertia Control-Based Coefficient Diagram Method

HOSSAM ALI[1,2], GABER MAGDY[2,3], BINBIN LI[1], (Member, IEEE), G. SHABIB[2,4], ADEL A. ELBASET[5], DIANGUO XU[1], (Fellow, IEEE), AND YASUNORI MITANI[3], (Member, IEEE)

[1]School of Electrical Engineering and Automation, Harbin Institute of Technology, Harbin 150006, China
[2]Department of Electrical Engineering, Faculty of Energy Engineering, Aswan University, Aswan 81528, Egypt
[3]Department of Electrical and Electronics Engineering, Kyushu Institute of Technology, Fukuoka 804-8550, Japan
[4]Higher Institute of Engineering and Technology, King Marriott, Alexandria 23713, Egypt
[5]Department of Electrical Engineering, Faculty of Engineering, Minya University, Minya 61517, Egypt

Corresponding author: Binbin Li (libinbin@hit.edu.cn)

This work was supported in part by the National Natural Science Foundation of China under Grant 51720105008, and in part by the State Key Laboratory of Operation and Control of Renewable Energy and Storage Systems.

ABSTRACT Renewable energy sources (RESs) are growing rapidly and highly penetrated in microgrids (MGs). As a result of the replacement of the synchronous generators with a large amount of RESs, the overall system inertia might be dramatically reduced which negatively affected the MG dynamics and performance in face of uncertainties, leading to weakening of the MG stability, which considers being a serious challenge in such grids. Therefore, in order to cope with this challenge and benefit from a maximum capacity of the RESs, robust control strategy must be applied. Hence, in this paper, a new application of robust virtual inertia control-based coefficient diagram method (CDM) controller is proposed in an islanded MG considering high-level RESs penetration for enhancement the system's validity and robustness in face of disturbances and parametric uncertainties. The proposed controller's proficiency has been checked and compared with H-infinite controller using MATLAB/Simulink which approved that the CDM controller achieved superior dynamic responses in terms of accurate reference frequency tracking and disturbance reduction over H-infinite in all test scenarios. Thus, the proposed controller alleviates the difficulties of H-infinite controller such as the experience and necessary abilities to design the form of the weighting functions for the system. Consequently, the frequency stability is improved and approved that the proposed CDM-based virtual inertia controller can significantly support a low-inertia islanded microgrid against RESs and load fluctuations.

INDEX TERMS Virtual inertia control, renewable energy sources, coefficient diagram method (CDM), frequency control.

I. INTRODUCTION

Recently, there is a growing interest in integrating Renewable Energy Sources (RESs) into the electrical power grids as a future solution for the reduction of greenhouse gas emissions generated by conventional power plants, such as carbon dioxide and nitrogen oxide which have bad environmental consequences [1]. As a result, several conventional generation units are being replaced by the concept of Distributed Generators (DGs)/ RESs such as solar, wind energy, microturbine, and small thermal power plants. In other words, small power generation sources such as wind turbines and photovoltaic (PV) are connected to close distributed sites. Although, this concept has a lot of merits such as reduction of the voltage droop and transmission system losses, and enhancing system reliability, it has some impacts on the performance of the modern power systems such as lack of system inertia [2], [3].

Microgrid (MG) has considered providing an appealing infrastructure for overcoming the challenges of integrating RESs/DGs to the grid [4]. Where the MG acts as a single controllable entity with respect to the grid and that connects and disconnects from such grid to enable it to operate in

both grid-connected mode or islanded mode [5]. During grid-connected mode, the MG receives power from both the utility grid and the DGs. Moreover, under grid-connected mode, a major portion of the real power required for the load is met by the DGs connected to the MG and the remaining few portions and the variation in the real power demand is met by the grid [6]. On the other hand, during islanded mode, the shedding of load/generation is carried out to reserve power balance. Thus, the critical loads are made to receive quality power at all time and the remaining loads are made to undergo load shedding [6]. Therefore, there are some researches have addressed the challenges of the MG operation from the perspective of grid-connected mode as in [7]–[9], and from the perspective of islanded mode as in [10]–[12]. Based on the aforementioned studies, MGs control in an islanded mode is more difficult than the grid-connected mode, because voltage and frequency regulation of the MGs in grid-connected mode are initially supported by the main utility grid. In the islanded mode, some MG resources should compensate the fluctuation in load and generation (wind power and solar irradiation). Hence, preserving the frequency stability of the islanded MGs is one of the important challenges, which is addressed in this study.

With increasing the penetration level of RESs into MGs, the RESs can bring significant impacts to the system inertia. Where the RESs coupled into the power grids through power electronic devices (i.e., inverters and converters), which reduce the overall system inertia that is considered the main source of stability. Accordingly, the inverter-based RESs will cause high-frequency fluctuations in compare with the conventional power systems [13], [14]. Therefore, if the penetration level of RESs become larger, it will raise new concern about the islanded MG stability, reliability, and efficiency. Hence, the frequency control becomes more difficult in case of any mismatch between the power generation and the load demand [2], [15]. A promising solution towards stabilizing such grids is to emulate the behavior of synchronous generator virtually into MGs for improving the system inertia, stability, and resiliency. It is known as Virtual Synchronous Generator (VSG) that emulates the action of the prime movers (e.g., inertia characteristic) [1]. Virtual inertia control is considered a specific case of VSG implementation, where the action of the prime mover is emulated for frequency stability support. Therefore, the virtual inertia control is implemented based on the function of the Rate of Change of Frequency (RoCoF) to give additional active power to the setpoint, thus enhance the frequency stability of the islanded MG [16], [17].

During the past few years, different control strategies have been implemented to virtual inertia control for frequency stability improvement of MGs [13], [18], [18], [20], [21]. Among them, conventional controllers such as proportional-Integral-Derivative (PID) and PI controllers [13], [18], Fuzzy Logic Controller (FLC) [19], [20], Model predictive control [21]. In addition, robust control techniques have recently received more interest in MG applications in order to solve problems related to model uncertainty during the synthesis procedure effectively [22]. Some research and studies on robust control applications for various MGs have been stated in [23]–[26]. a μ-based robust controller is proposed for frequency regulation in an autonomous MG in [23]. In [24], a robust controller-based H-infinite technique has been implemented for power-sharing in MGs with low-inertia wind and PV generators. Also, a robust controller-based H-infinite technique has been proposed for the LFC of the hybrid generation system in [25]. While, H-infinite and μ-synthesis robust control techniques are applied to improve the secondary frequency control loop (i.e., Load Frequency Control (LFC)) in [26]. Moreover, it is revealed that the μ-synthesis strategy provides better performance than the H-infinite control scheme in the presence of structured/parametric uncertainties. In spite of the robust control techniques [23]–[26] gave a decent dynamic response, they depend on the control designer experience by choosing the suitable weight functions. Also, the order of designed state feedback H-infinite controllers is normally bigger than the order of the controlled system which considers being demerits of this controller [27], [28].

Motivated by the aforementioned observations regarding the robust control techniques, this research presentsa new control approach so-called as Coefficient Diagram Method (CDM), which will be applied as a robust virtual inertia controller for improving an islanded MG's frequency stability. CDM well-thought-out as a Polynomial method (i.e., algebraic design approach) where a unique outline called coefficient diagram can be obtained algebraically from the characteristic polynomial by solving a Diophantine equation [29]. The CDM design is theoretically proven to be equivalent to LQ design with proper state increment. Thus, CDM can be considered an ''improved LQG'', because the order of the controller is smaller and weight selection rules are also given [30]. CDM is well adapted to load frequency control designs in both single and multi-area power systems as investigated in [31] and [32].

Therefore, in this paper, the robust virtual inertia control for an islanded MG has been designed based on the proposed CDM controller. Where the parameters and the polynomials of CDM controller have been developed based on the dynamic model of the islanded MG. Moreover, the effects of the physical constraints such as Generation Rate Constraint (GRC) and speed governor dead-band are taken into consideration [22]. The islanded MG with the proposed CDM controller has been tested through the effects of uncertainties (due to governor and turbine parameters variation, RESs and load perturbations). To validate the effectiveness and robustness of the proposed virtual inertia control-based CDM controller, a comparison is made between the proposed CDM controller and the robust controller-based H-infinite technique applied in [4] utilizing MATLAB/Simulink software.

The distinguished features of the proposed robust CDM control technique in this paper over the existing control techniques in the islanded MG is that:

i. The CDM control approach is handled the MG system inertia as a bounded sector of uncertainties;
ii. The CDM control approach has treated the variations of RESs and load as a bounded sector of disturbances;
iii. A robust virtual inertia controller-based CDM is designed to minimize an islanded microgrid frequency deviations, thus improving MG stability and resilience.

The remainder of the paper is organized as follows: in section II the description of the dynamics of the islanded MG is considered. A brief review of virtual inertia control concept is described in section III. Section IV provides the proposed control strategy for design the virtual inertia control. Simulation results and general remarks are presented in section V. Finally, the paper is concluded in section VI.

II. SYSTEM DYNAMICS OF AN ISLANDED MICROGRID

An islanded MG is considered as a test system to design and validate the proposed virtual inertia control strategy-based the CDM controller. The MG is a group of interconnected loads and DGs (e.g., solar, wind, wave, microturbine, and small hydroelectric power plants) [5]. This study focuses on the islanded MG that consists of a thermal power plant with 12 MW, wind power with 7 MW, solar power with 4 MW, and domestic loads with 15 MW. The system base is 20 MW. The simplified model of the islanded MG with the proposed virtual inertia control strategy based on the CDM controller is shown in Fig. 1.

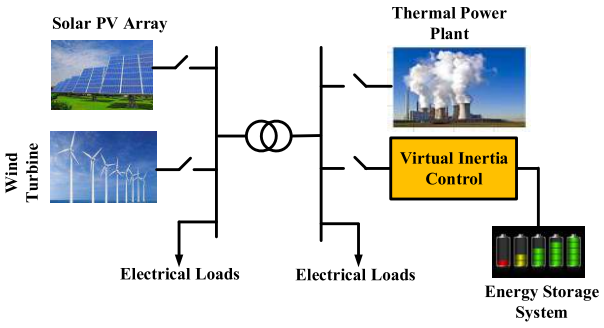

FIGURE 1. Simplified schematic of an islanded MG.

The nonlinear model of the studied islanded MG considering RESs and the proposed virtual inertia control-based the CDM controller is shown in Fig. 2, and the MG parameters are given in Table 1. This study has taken into consideration low-order dynamic response models for RESs because they are considered sufficient for frequency stability analyzing of MGs, according to the references [4], [18], and [22]. Therefore, the wind power variation (ΔP_{Wind}), the solar power variation (ΔP_{Solar}), and the load power variation (ΔP_L) are assigned as the disturbances to the studied MG. Also, the effects of the physical constraints such as GRC and the maximum/minimum limit of the valve gate (i.e., Governor Dead-band (GDB) are taken into consideration to obtain an accurate perception for the islanded MG. The GRC for the non-reheat thermal power plant is specified as 20% p.u. MW/minute [33]. Moreover, the maximum and minimum limits (V_U, V_L) restrict the valve opening/closing. The islanded MG frequency deviation considering the effect of primary frequency control, secondary frequency control (i.e. LFC), and inertia control can be expressed as:

TABLE 1. Dynamic parameters of the islanded MG (Fig. 2).

Parameters	Value
Microgrid damping coefficient, D (p.u.MW/Hz)	0.015
equivalent inertia constant, H (p.u. MWs)	0.083
governor time constant, T_g (s)	0.1
turbine time constant, T_t (s)	0.4
Wind turbine time constant, T_{WT} (s)	1.5
Solar system time constant, T_{PV} (s)	1.8
speed droop characteristic, R (Hz/p.u.MW)	2.4
Integral control variable gain, K_I (s)	0.05
Virtual inertia control gain, K_{VI} (s)	0.5
Virtual inertia time constant, T_{VI} (s)	10
Maximum limit of valve gate, V_U (p.u. MW)	0.3
Minimum limit of valve gate, V_L (p.u. MW)	-0.3
Generation Rate Constraints, GRC %	20%
Frequency, F (Hz)	50
Integral control variable gain, K_I (s)	0.05

$$\Delta f = \frac{1}{2Hs+D}\left(\Delta P_m + \Delta P_{WT} + \Delta P_{PV} + \Delta P_{Inertia} - \Delta P_L\right) \tag{1}$$

where:

$$\Delta P_m = \frac{1}{1+sT_t}\left(\Delta P_g\right) \tag{2}$$

$$\Delta P_g = \frac{1}{1+sT_g}\left(\Delta P_c - \frac{1}{R}\Delta f\right) \tag{3}$$

$$\Delta P_{WT} = \frac{1}{1+sT_{WT}}\left(\Delta P_{Wind}\right) \tag{4}$$

$$\Delta P_{PV} = \frac{1}{1+sT_{PV}}\left(\Delta P_{Solar}\right) \tag{5}$$

III. VIRTUAL INERTIA CONTROL STRATEGY

In conventional power systems, the synchronous generators are responsible for providing inertia to the grid through the stored kinetic energy in their rotating mass. The intrinsickinetic energy of the synchronous generators plays an important role in power system stability. On the other hand, in MGs, the RESs may replace many synchronous generators, thus the inertia of MGs decreases due to lack of any rotating mass, which is the main source of inertia [1]. Therefore, with increasing the penetration level of RESs into the MGs, the influence of low system inertia on the dynamic system performance and stability increases. Moreover, the intermittent nature of the RESs causes many control problems such as frequency instability problem, which may be limiting

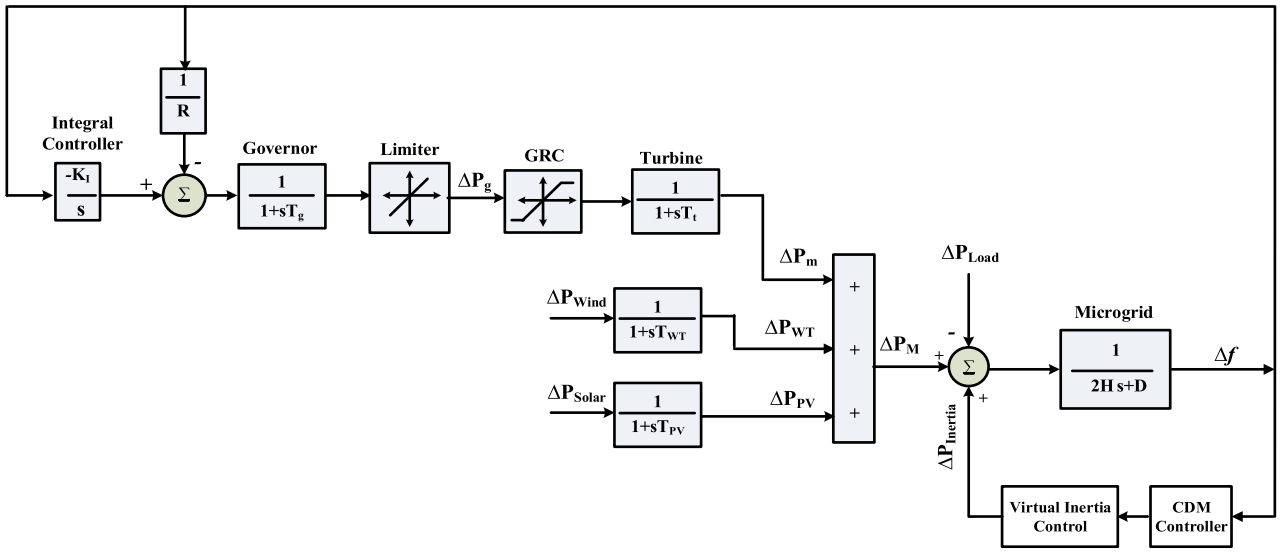

FIGURE 2. Frequency response model of the islanded MG.

their high penetration [18]. As a result, MGs have become more susceptible to the disturbances than traditional power systems, thus are facing some of the disturbances such as; large frequency fluctuations, sudden load shedding, forced islanding incidents, and short-circuit faults with long clearing times [34]. Therefore, lack of inertia response resulting from the high penetration level of RESs in the islanded MG can be compensated by adding active power to the set point, which is simulated by the virtual inertia control strategy. Where the virtual inertia control strategy aims to emulate the activity of the prime mover to support the frequency stability of the islanded MG. Moreover, it is based on the derivative control, which calculates the RoCoF to add a compensation active power to the set-point of the islanded MG during high-level RESs penetration and contingencies [4], [18].

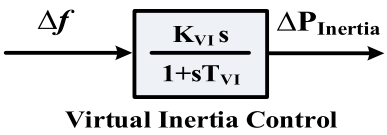

FIGURE 3. Structure of the designed virtual inertia control.

In this study, the energy storage system (ESS) has been used to create the virtual inertia power for emulating the kinetic energy stored in rotating mass of a real synchronous generator in large power systems. Therefore, the virtual control strategy law for emulating virtual inertia power in the form of Laplace based on the per-unit system is shown in Fig. 3. Where the proposed virtual inertia control system gives the desired power to the MG during the deviation of frequency and essentially when the RESs are highly penetrated as follows [34].

$$\Delta P_{Inertia} = \frac{K_{VI}}{1 + sT_{VI}} \left[\frac{d(\Delta f)}{dt} \right] \tag{6}$$

where, T_{VI} is the time constant-based virtual inertia to emulate the dynamic control of the energy storage system in the studied MG, and K_{VI} is the gain of virtual inertia control in the islanded MG.

IV. VIRTUAL INERTIA CONTROL BASED COEFFICIENT DIAGRAM METHOD

A. BASICS OF CDM

In general, the control system design problem depends on the selection of a proper controller which usually required to be designed under some practical limitations by considering the plant dynamics and performance specifications. A suitable controller is desired to have a minimum degree, minimum phase (if possible) and stable.

It is not difficult to define the characteristic polynomial from stability and response specification, but it is very difficult to choose it with the guarantee of robustness. Coefficient Diagram Method (CDM) is one of the polynomial methods combining classical and modern control theories, which is derived by allowing the use of the previous experience and knowledge of the controller design to solve this problem. The historical background is given in [35].

Besides the CDM algebraic nature, this method also utilizes a coefficient diagram instead of the Bode diagram, and its theoretical basis is constituted using condition for stability by Lipatov and Sokolov [36]. The standard block diagram of the CDM design for a single-input-single-output (SISO) linear time-invariant system is shown in Fig. 4, Where N(s) is numerator polynomial, and D(s) is denominator polynomial of the plant transfer function. Also, A(s) is considered as forwarding denominator polynomial, F(s) and B(s) are considered as reference numerator and feedback numerator polynomials of the controller, respectively. Since the controller's transfer function has two numerators, it implies a

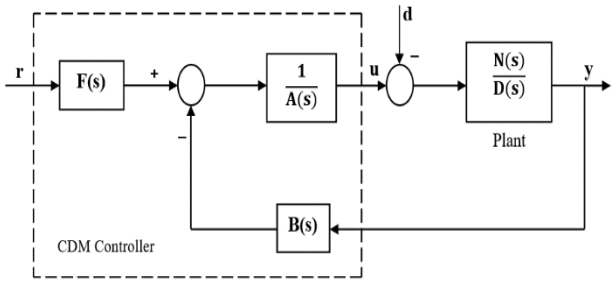

FIGURE 4. Block diagram of the CDM control system.

2DOF system structure [31]. Better performance can be projected when using a 2DOF structure, as it can focus on both disturbance rejection and tracking the desired reference signal [37].

The transfer function of a linear time-invariant SISO plant is expressed as:

$$G(s) = \frac{N(s)}{D(s)} = \frac{a_m s^m + a_{m-1}s^{m-1} + \cdots + a_1 s + a_0}{b_n s^n + b_{n-1}s^{n-1} + \cdots + b_1 s + b_0} \quad (7)$$

In CDM, the characteristic polynomial takes the following generic format.

$$P(s) = a_n s^n + \cdots + a_1 s + a_0 = \sum_{i=0}^{n} a_i s^i, \quad a_i > 0 \quad (8)$$

This is also called as the target characteristic polynomial where a_i are the polynomial $P(s)$ coefficients.

In this method, d is the external disturbance signal; r is taken as the reference input to the system; u as the controller signal; and y is the output of the CDM control system which given by:

$$y = \frac{N(s)F(s)}{P(s)}r + \frac{A(s)N(s)}{P(s)}d \quad (9)$$

where P(s) can be alternatively defined as:

$$P(s) = A(s)D(s) + B(s)N(s) \quad (10)$$

where $A(s)$ and $B(s)$ are considered as the control polynomial and is defined as:

$$A(s) = \sum_{i=0}^{P} l_i s^i, \quad B(s) = \sum_{i=0}^{q} k_i s^i \quad (11)$$

Since l_i and K_i are CDM controller parameters. For practical realization, the condition $p \geq q$ must be fulfilled.

The actuating signal u for the closed loop is

$$u = \frac{D(s)F(s)}{P(s)}r + \frac{A(s)D(s)}{P(s)}d \quad (12)$$

To acquire the characteristic polynomial $P(s)$, the controller polynomials from Eq. (11) are substituted in Eq. (10) and is given as:

$$P(s) = \sum_{i=0}^{P} l_i s^i D(s) + \sum_{i=0}^{q} k_i s^i N(s) = \sum_{i=0}^{n} a_i s^i, \quad a_i > 0 \quad (13)$$

where the summation of the right hand-formula can be expanded in the form of equation (8), after remodeling the left-hand formula by combining all of the coefficients for the same (s) operator order.

For designing CDM controller it needs some specifications parameters with respect to the characteristic polynomial coefficients such as the equivalent time constant (τ) (which gives the speed of closed loop response), the stability indices (γ_i) (which give the stability and the shape of the time response), and the stability limits (γ_i^*) [29]. The relations between these parameters and the coefficients of the characteristic polynomial (a_i) can be described as follows:

$$\gamma_i = \frac{a_i^2}{a_{i+i}a_{i-1}}, \quad i \in [1, n-1], \ \gamma_0 = \gamma_n = \infty \quad (14)$$

$$\tau = \frac{a_1}{a_0} \quad (15)$$

$$\gamma_i^* = \frac{1}{\gamma_{i-1}} + \frac{1}{\gamma_{i+1}}, \quad i \in [1, n-1] \quad (16)$$

There is a relationship between the equivalent time constant (τ), and the actuating signal. For large τ, the time response slows down and the magnitude of the actuating signal becomes smaller. Therefore, choosing the appropriate time equivalent constant (τ) is one of the important steps in the design procedure [38]. As mentioned in [39] equivalent time constant (τ) and stability indices (γ_i) are chosen as:

$$\tau = \frac{t_s}{2.5 \approx 3} \quad (17a)$$

where t_s is the user specified settling time.

$$\gamma_i = [2.522\ldots] \quad (17b)$$

The above γ_i values are from the Manabe's standard form [40] and these values can be changed by the designer as per the requirement in order to satisfy the desired performance.

Finally, the characteristic polynomial given in equation (8) can be rewritten to obtain target characteristic polynomial in terms of the key parameters (τ, γ_i) and a_0 by the relation:

$$P_{target} = a_\circ \left[\left\{ \sum_{i=2}^{n} \left(\prod_{j=1}^{i-1} \frac{1}{\gamma_{i-j}^j} \right) (\tau s)^i \right\} + \tau s + 1 \right] \quad (18)$$

where $P_{(s)} = P_{target(s)}$

B. STABILITY CRITERION

From the Routh-Hurwitz stability criterion [41], the stability condition for the 3rd order system is given as:

$$a_2 a_1 > a_3 a_0. \quad (19a)$$

If it is expressed by stability index,

$$\gamma_2 \gamma_1 > 1 \quad (19b)$$

The stability condition for the fourth order system is given as:

$$a_2 > (a_1/a_3)a_4 + (a_3/a_1)a_0, \quad (20a)$$

$$\gamma_2 > \gamma_2^* \quad (20b)$$

For the system higher than or including 5th degree, Lipatov and Sokolov [36] gave the sufficient condition for stability and instability in several different forms. The conditions most suitable to CDM can be stated as follows; "The system is stable if all the partial 4th order polynomials are stable with the margin of 1.12. The system is unstable if some partial 3rd order polynomial is unstable."

Thus, the sufficient condition for stability is given as:

$$a_i > 1.12\left[\frac{a_{i-1}}{a_{i+1}}a_{i+2} + \frac{a_{i+1}}{a_{i-1}}a_{i-2}\right], \tag{21a}$$

$$\gamma_i > 1.12\gamma_i^*, \quad \text{for all } i = 2 \sim n-2 \tag{21b}$$

The sufficient condition for instability is given as:

$$a_{i+1}a_i \leq a_{i+2}a_{i-1}, \tag{22a}$$

$$\gamma_{i+1}\gamma_i \leq 1, \quad \text{for some } i = 1 \sim n-2 \tag{22b}$$

Consequently, based on the past equations it can sum up that the range of a parameter (i) depends mainly on the order of the controlled system.

C. CDM CONTROLLER DESIGN PROCEDURE

The CDM design procedure is summarized as follows.

i. an implementation of the plant mathematical model, in polynomial format, is required.
ii. selecting a proper controller polynomial structures, $A(s)$ and $B(s)$ based on system specifications and the disturbance rejection properties.
iii. Constructing the characteristic equation $P(s)$ in the polynomial form as equation (10).
iv. Specifying a suitable equivalent time constant (τ) and stability indices (γ_i) as mentioned previously in section B.
v. The target characteristic equation is established concerning the desired dynamic performance.
vi. Finally, the robust controller coefficients are obtained by comparing $P_{(s)}$ and $P_{target(s)}$.

The flowchart for coefficient diagram algorithm procedure is outlined as shown in Fig. 5.

D. CDM DESIGN FOR VIRTUAL INERTIA CONTROL

The aim of the controller is to achieve the desired performance within the bound of the disturbance. Following the design procedure, according to values of MG parameters in table.1 the closed loop transfer function of the plant model can be defined as follows:

$$N(s) = 150.6s + 15.06,$$
$$D(s) = s^4 + 12.39s^3 + 23.6s^2 + 60.09s + 6.501$$

from Eq. (11) the CDM controller polynomials are chosen in the form of:

$$A(s) = l_2s^2 + l_1s + l_0, \quad B(s) = k_2s^2 + k_1s + k_0$$

And, the parameters of the CDM controller are set as follows:

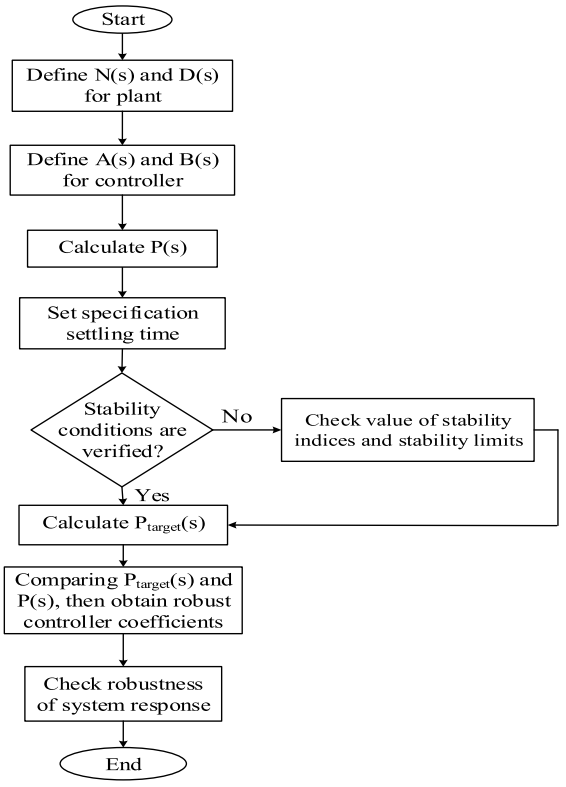

FIGURE 5. A simplified flowchart for coefficient diagram method.

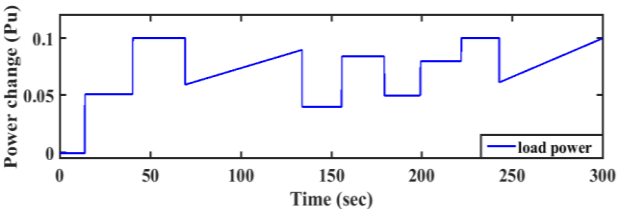

FIGURE 6. Power pattern for random load demand.

The time constant can be taken as $\tau = 1.86$ sec, assuming $a_0 = 1$. The stability indices (γi) are determined as:

$$\gamma_i = [1.927, 1.39, 0.431, 0.792, 1.46], \quad i \in [1, 5], \quad \gamma_0 = \gamma_6 = \infty$$

The stability index γ_i is chosen different from the standard form of CDM [34] in order to decrease the nonlinear effect on the time-response of the controlled system.

And the stability limits (γ_i^*) are:

$$\gamma_i^* = [1.24, 3.04, 3.58, 1.95, 0.8], \quad i \in [1, 5]$$

Further, $P_{target}(s)$ is calculated as follows:

$$P_{\text{target}}(s) = 0.7s^6 + 12.17s^5 + 59.9s^4 + 249.4 \times 10^3 s^3 + 24.96 \times 10^3 s^2 + 258.03 \times 10^3 s + 1$$

And by choosing l_0=0.1, then the controller parameters are obtained as:

$$B(s) = 1125s^2 + 15.436 \times 10^3 s + 71.335 \times 10^3, \quad i \in [1, 4]$$
$$A(s) = 0.7s^2 + 3.5s + 0.1, \quad i \in [1, 4]$$

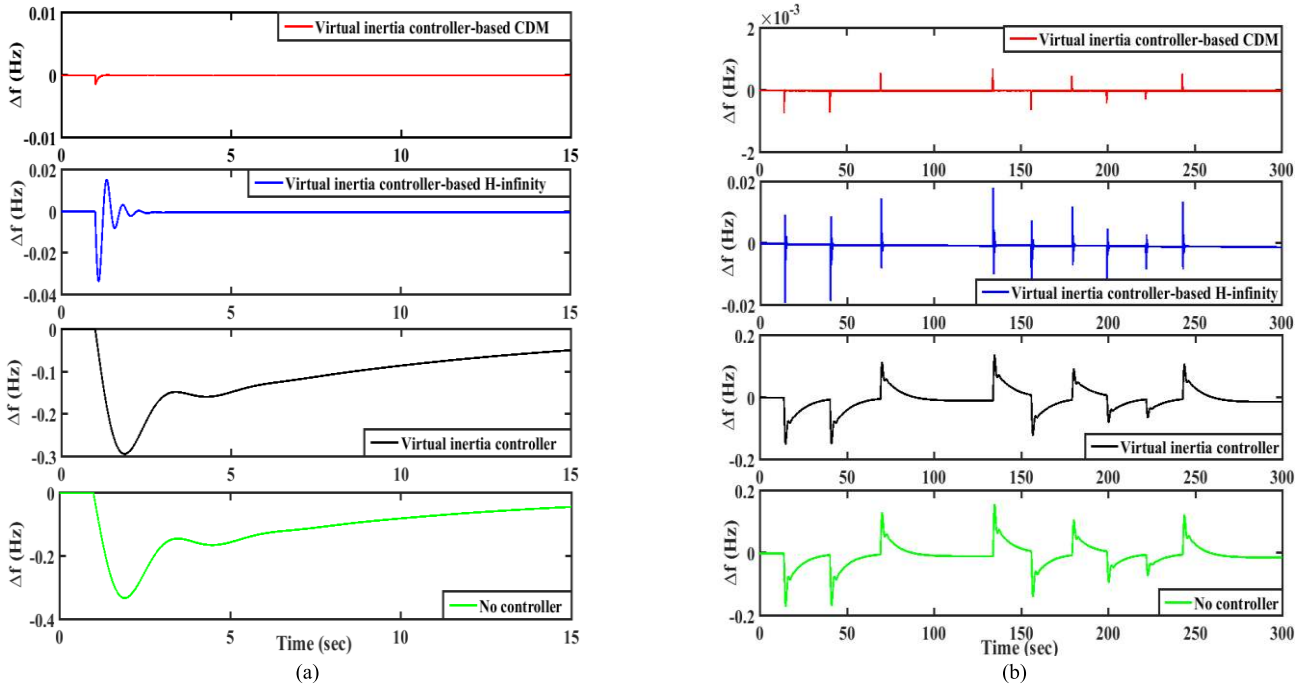

FIGURE 7. The MG frequency deviation for scenario A; (a) 10 % SLP, (b) random load.

Notice that the structure of proposed virtual inertia controller-based CDM is much simpler than the designed H-infinity high order robust controller as given in Appendix A; moreover, there is no need for controller order reduction which is a great advantage.

V. SIMULATION RESULTS AND DISCUSSION

The simulation results of the islanded MG have been carried out using Matlab/Simulink to test and evaluate the proposed virtual inertia control based on the CDM controller. Moreover, the performance of the proposed control strategy is compared with a robust controller-based H-infinite technique that implemented in [4] under the nature variety of the RESs and system parameters variations to validate the effectiveness of the proposed CDM controller. Thus, the frequency stability analysis of the MG is implemented under different operating conditions through the following scenarios:

A. PERFORMANCE EVALUATION OF THE MG WITH NOMINAL SYSTEM PARAMETERS

In this section, the performance of the islanded MG with the proposed virtual inertia control based on the CDM controller is investigated by using the nominal system parameters as given in Table 1. This studied case is divided into two scenarios, which are implemented with/without the effect of RESs uncertainties.

Scenario A: In this scenario, the performance of the studied MG with the proposed virtual inertia control-based CDM controller is tested and evaluated by applying different load

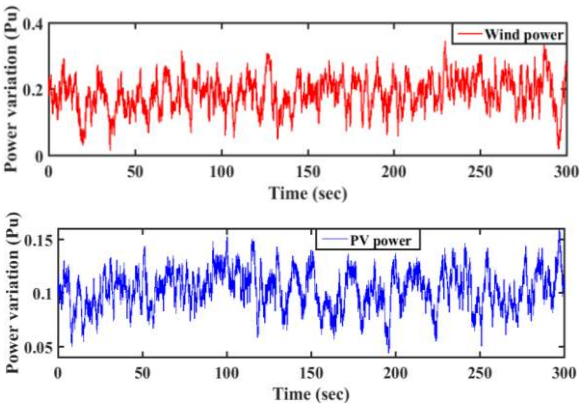

FIGURE 8. Power variations pattern of wind and solar generations.

patterns; a 10% Step Load Perturbation (SLP) at time t=1 sec, and a random load demand as shown in Fig.6. Fig. 7 displays the frequency deviation of the studied MG with the different control strategies; the proposed virtual inertia control-based CDM, virtual inertia control-based H-infinity technique, virtual inertia control, and without virtual inertia control (i.e., no controller) under the impact of a 10 % SLP as shown in Fig. 7 (a), and under the impact of the random load as shown in Fig. 7 (b). From Fig. 7, it is clear that the proposed virtual inertia control-based CDM controller gives superior performance and more reduction of the frequency excursions compared to other control strategies. Where the frequency deviation of the MG without virtual inertia controller has been maintained within ±0.35 Hz, ±0.18 Hz, in the cases of 10%

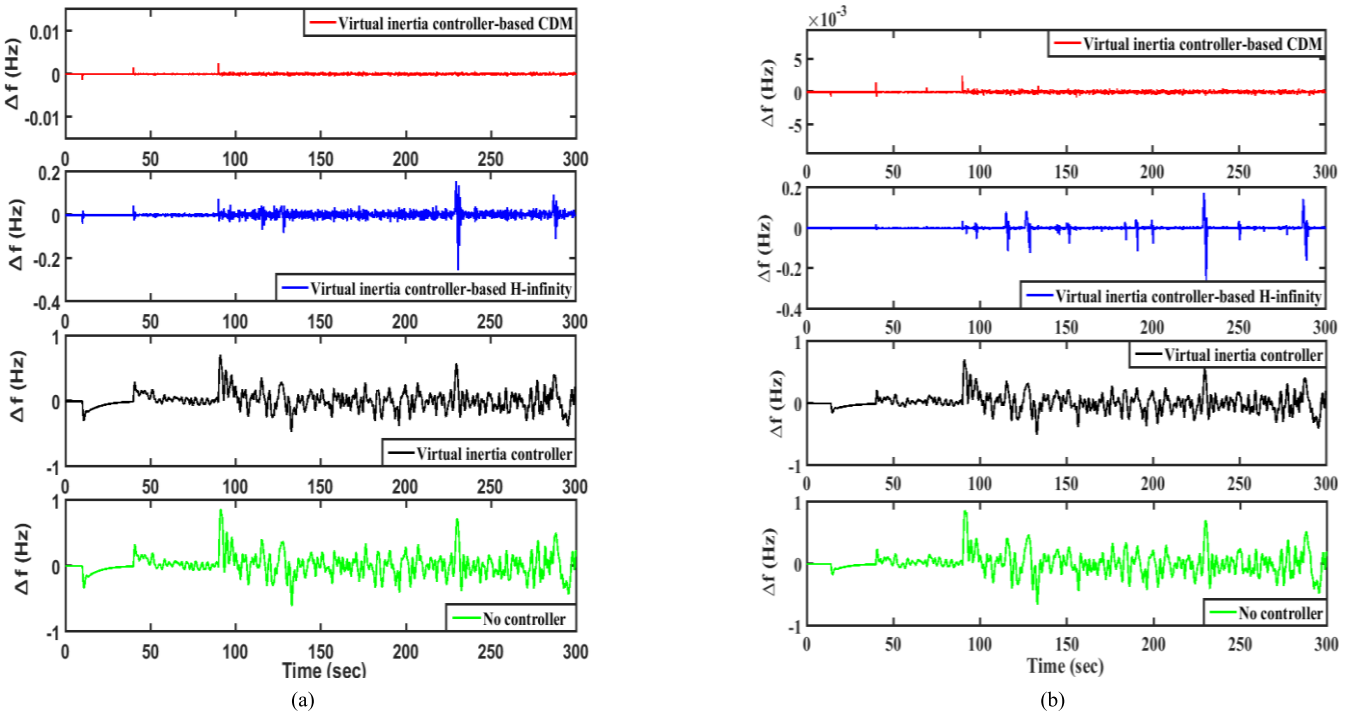

FIGURE 9. The MG frequency deviation for scenario B; (a) 10 % SLP, (b) random load.

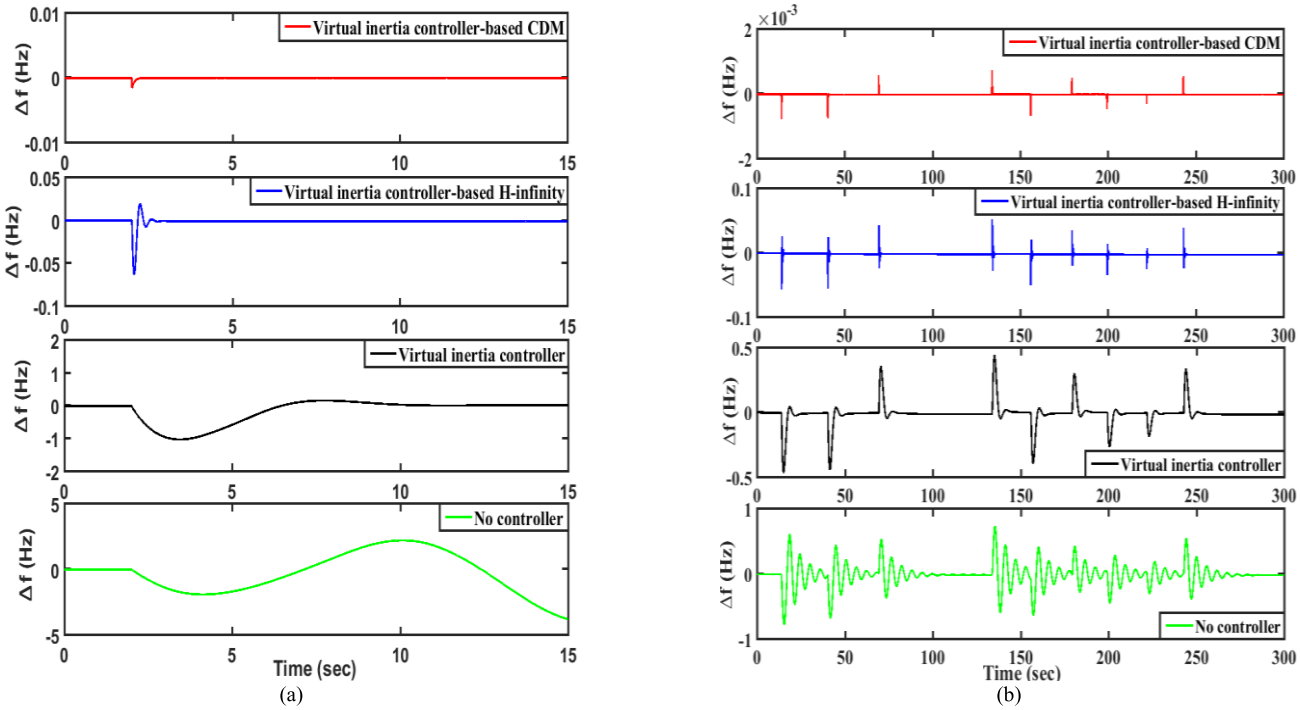

FIGURE 10. The MG frequency deviation for scenario C; (a) 10 % SLP, (b) random load.

SLP, and random load respectively. While the studied MG with the virtual inertia controller gives a frequency change of ±0.30 Hz during the connection of a 10% SLP at t = 1 sec, and ±0.18 Hz during random load connecting. On the other hand, the frequency deviation of the MG with the proposed virtual inertia controller-based CDM has been maintained within a ±0.003 Hz in that cases, while the studied MG with the virtual inertia controller-based H-infinite technique

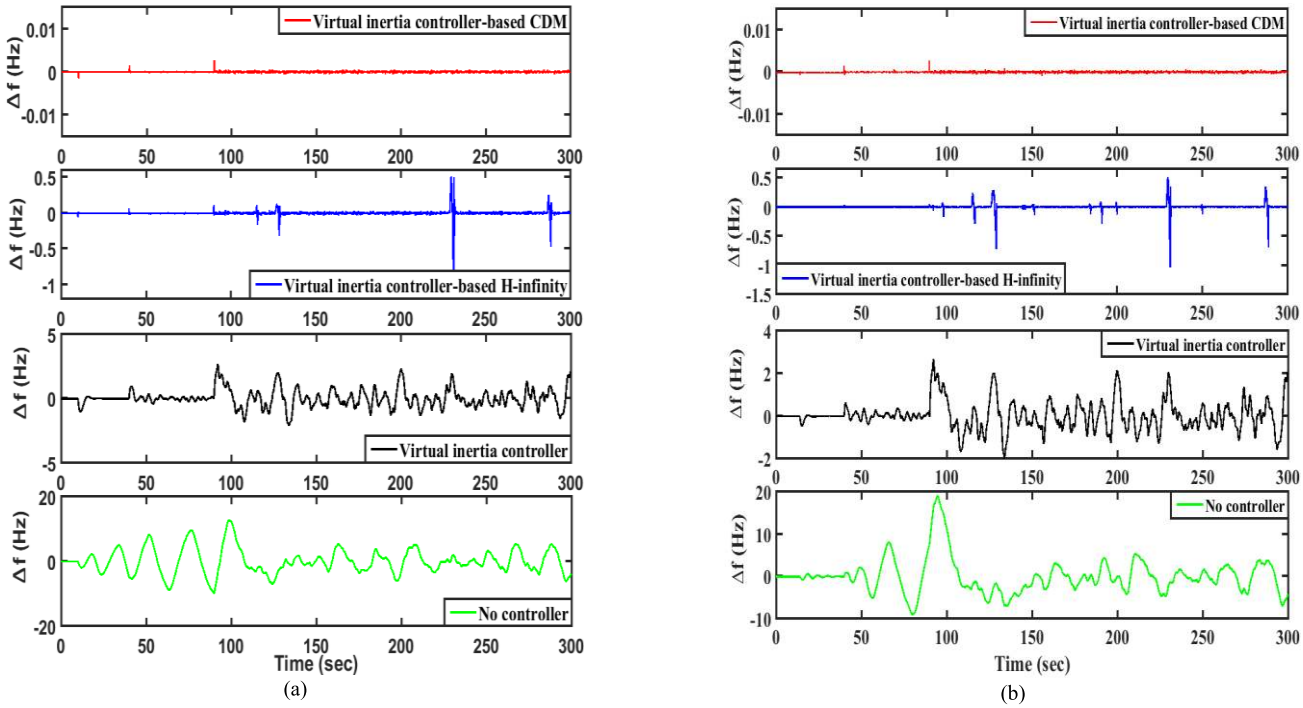

FIGURE 11. The MG frequency deviation for scenario D; (a) 10 % SLP, (b) random load.

can maintain the frequency deviation within a ±0.035 Hz. Thus, the frequency response of the MG with the proposed control strategy based on CDM is faster, has a lower steady-state error, and better damped than that by using the virtual inertia controller-based H-infinity technique.

Scenario B: The main target of this scenario is to evaluate the performance of the studied MG with the proposed virtual inertia control-based CDM controller under the effect of the RESs uncertainties. Therefore, the studied MG is examined by implementing wind power at t = 90 sec, PV solar power at t = 40 sec, and by applying different load patterns; a 10% Step Load Perturbation (SLP) at time t=10 sec, and a random load demand as shown in Fig.6. Fig. 8 shows the variation patterns of wind and solar power. Fig. 9 shows the frequency deviation response of the studied MG considering high penetration of RESs with different control strategies under the impact of a 10 % SLP as demonstrated in Fig. 9 (a), and under the impact of the random load as demonstrated in Fig. 9 (b). From the simulation results, the frequency deviation of the MG with the virtual inertia control based on H-infinity technique has been maintained within ±0.29 Hz during connection of wind power at t=230 sec in both cases of load variation, while the frequency deviation of the studied MG with the proposed control strategy-based CDM has been maintained within ±0.005 Hz when the wind farm is connected at t=90 sec at both cases of load variation. However, it is clear that in the presence of the random load demand the MG response with the H-infinity controller became oscillated in compare with the proposed CDM controller. Therefore, the studied MG considering high penetration of RESs with the proposed control strategy is significantly more stable and faster, compared to that with H-infinity technique as shown in Fig. 9. Alternatively, the frequency response of the studied MG with/without the virtual inertia control fluctuate severely due to critical inertia reduction resulting from high penetration of RESs, thus give an unsatisfactory performance.

B. PERFORMANCE EVALUATION OF THE MG WITH A VARIATION OF SYSTEM PARAMETERS

In this section, the robustness of the studied MG with the virtual inertia control based on the CDM controller against parameters uncertainty is evaluated by drastically changing the system parameters of the MG. This studied case is also divided into two scenarios, which are employed with/without the effect of high fluctuation of RESs.

Scenario C: To assess the behavior of the MG under the severe test scenario, both turbine, and thermal generation governor time constants are increased to $T_g = 0.12$ sec, and $T_t = 0.975$ sec respectively. This situation can occur when off-line changing the practical turbine and governor parameters. Besides, the damping coefficient value is increased to D = 0.0195 (p.u.MW/Hz) (i.e., increased by 35 % of its nominal value). Subsequently, these values are considered to lead the thermal power plant and MG system to unstable mode. Furthermore, the islanded MG is tested under the critical condition of low system inertia (i.e., reduced to 30% of its nominal value). The load demand variation pattern is assumed to be as described in scenario (A). Fig. 10, demonstrates the MG frequency deviation under the severe case of uncertainty. It has been depicted that the performance of

$$K(s) = \frac{2.189 \times 10^4 s^3 + 2.508 \times 10^6 s^2 + 4.846 \times 10^7 s + 3.177 \times 10^4}{s^4 + 261.8 s^3 + 1.525 \times 10^4 s^2 + 154.4 s + 0.01941}$$

the MG without virtual inertia controller (i.e., no controller) oscillates severely due to system uncertainties in both cases of a load change, thus give an unsatisfactory performance. While a desirable performance is detected by the virtual inertia control based CDM controller comparing the other two cases; where the frequency deviation of the studied MG with the virtual inertia controller has been maintained within ±0.95 Hz, ±0.48 Hz in the cases of 10% SLP, and random load respectively, and H-infinity controller can maintain the frequency deviation within a ±0.065 Hz in that cases. As well, with the proposed virtual inertia controller-based CDM the frequency deviation has been maintained within ±0.002 Hz during both load change cases. In this case of study, it has been obviously verified that the response of the MG with the proposed control strategy is more convenient and superior than using other controllers.

Scenario D: The robustness of the proposed virtual inertia control-based CDM controller is examined in this extreme scenario test based on the high integration of RESs as mentioned in scenario (B), and severe variations of system parameters as considered in scenario (C). From Fig. 11, it can be realized that the MG with the conventional LFC (i.e., without virtual inertia controller) cannot endure the frequency deviation in face of multiple changes in RESs and load, thus gives a non-reliable performance. Also, the MG with the virtual inertia control loops gives a large transient frequency deviation and larger oscillating overshoots, leading to frequency fluctuation with a higher range. On the other hand, the virtual inertia control-based CDM controller can effectively cope with the system uncertainties, maintain the system frequency to its nominal value (50 Hz). While the virtual inertia control-based H-infinity technique significantly affected by the RESs uncertainty as shown in the glance of t = 230 sec in Fig. 11, as it has been tested under the impact of a 10 % SLP as shown in Fig. 11 (a), and under the impact of the random load as shown in Fig. 11 (b). Where the system frequency deviation in that cases reach to un acceptable value about ±1.2 Hz, thus leading to system instability and collapse. In contrast, the proposed virtual inertia control-based gives a superior performance where has been successfully treated this contingency. As a result, this considers being great evidence for the robustness and effectiveness of the proposed control strategy based CDM controller over the other comparative methods. Hence, the designed robust CDM control approach may have a great potential in the virtual inertia control aspects for MGs.

VI. CONCLUSION

This paper presents a new frequency control concept based on the virtual inertia control in the aim of support the frequency control loops of an islanded microgrid considering the high penetration level of renewable energy sources (RESs). Moreover, the proposed virtual inertia controller is based on a robust control strategy, namely coefficient diagram method (CDM) controller that has a simple structure compared to others robust controllers. Therefore, the performance of the proposed virtual inertia control-based CDM controller is compared with that a robust controller-based H-infinity technique under the nature variety of the RESs and system parameters variations to validate the effectiveness of the proposed CDM controller. The simulation results are carried using MATLAB/Simulink software. Thus, the results emphasized the superior robustness of the proposed virtual inertia control-based CDM controller in comparison to the robust controller-based H-infinity. In addition, the proposed controller has been able to handle high systemuncertainty and severe disturbances more efficiently. Finally, the proposed controller (i.e., CDM controller) could overcome the difficulties of the H-infinity technique.

APPENDIX

The designed robust controller-based H-infinite technique in [4].

- The transfer function of the designed -infinity controller with the full-order form was derived as:

$$K(s) = \frac{b_6 s^6 + b_5 s^5 + \cdots + b_1 s + b_0}{s^7 + a_6 s^6 + a_5 s^5 + \cdots + a_1 s + b_0} \quad (23)$$

Table. 2 shows the coefficients of the designed H-infinity controller in the form of equation (23).

TABLE 2. The coefficients of H-infinity based virtual inertia controller.

a_6	274.3	b_6	2.188×10^4
a_5	1.856×10^4	b_5	2.783×10^6
a_4	1.975×10^5	b_4	8.049×10^7
a_3	3.837×10^5	b_3	6.682×10^8
a_2	3979	b_2	1.215×10^9
a_1	1.635	b_1	1.148×10^6
a_0	0.0001473	b_0	240.2

- The transfer function of the reduced-order H-infinity controller was derived as K(s), shown at the top of this page.

REFERENCES

[1] H. Bevrani, T. Ise, and Y. Miura, "Virtual synchronous generators: A survey and new perspectives," *Int. J. Electr. Power Energy Syst.*, vol. 54, pp. 244–254, Jan. 2014.
[2] F. Blaabjerg, R. Teodorescu, M. Liserre, and A. V. Timbus, "Overview of control and grid synchronization for distributed power generation systems," *IEEE Trans. Ind. Electron.*, vol. 53, no. 5, pp. 1398–1409, Oct. 2006.
[3] J. Fang, H. Li, Y. Tang, and F. Blaabjerg, "Distributed power system virtual inertia implemented by grid-connected power converters," *IEEE Trans. Power Electron.*, vol. 33, no. 10, pp. 8488–8499, Oct. 2018.

[4] T. Kerdphol, F. S. Rahman, Y. Mitani, M. Watanabe, and S. Küfeoğlu, "Robust virtual inertia control of an islanded microgrid considering high penetration of renewable energy," *IEEE Access*, vol. 6, pp. 625–636, 2018.

[5] M. H. Khooban, T. Niknam, F. Blaabjerg, and T. Dragičević, "A new load frequency control strategy for micro-grids with considering electrical vehicles," *Electr. Power Syst. Res.*, vol. 143, no. 1, pp. 585–598, 2017.

[6] B. J. Brearley and R. R. Prabu, "A review on issues and approaches for microgrid protection," *Renew. Sustain. Energy Rev.*, vol. 67, no. 1, pp. 988–997, 2017.

[7] S. Bifaretti, S. Cordiner, V. Mulone, V. Rocco, J. L. Rossi, and F. Spagnolo, "Grid-connected microgrids to support renewable energy sources penetration," *Energy Procedia*, vol. 105, pp. 2910–2915, May 2017.

[8] M. El-Hendawi, H. A. Gabbar, G. El-Saady, and E.-N. A. Ibrahim, "Control and EMS of a grid-connected microgrid with economical analysis," *Energies*, vol. 11, no. 1, p. 129, 2018.

[9] W. Feng, K. Sun, Y. Guan, J. M. Guerrero, and X. Xiao, "Active power quality improvement strategy for grid-connected microgrid based on hierarchical control," *IEEE Trans. Smart Grid* , vol. 9, no. 4, pp. 3486–3495, Jul. 2018.

[10] W. Kang *et al.*, "Distributed secondary control method for islanded microgrids with communication constraints," *IEEE Access*, vol. 6, pp. 5812–5821, 2017.

[11] Q. Li, C. Peng, M. Wang, M. Chen, J. M. Guerrero, and D. Abbott, "Distributed secondary control and management of islanded microgrids via dynamic weights," *IEEE Trans. Smart Grid*, to be published. doi: 10.1109/TSG.2018.2791398.

[12] G. Agundis-Tinajero, J. Segundo-Ramírez, N. Visairo-Cruz, M. Savaghebi, J. M. Guerrero, and E. Barocio, "Power flow modeling of islanded AC microgrids with hierarchical control," *Int. J. Elect. Power Energy Syst.*, vol. 105, no. 1, pp. 28–36, 2019.

[13] P. F. Frack, P. E. Mercado, and M. G. Molina, "Extending the VISMA concept to improve the frequency stability in microgrids," in *Proc. 18th Int. Conf. Intell. Syst. Appl. Power Syst. (ISAP)*, Porto, Portugal, Nov. 2015, pp. 1–6.

[14] P. Babahajiani, Q. Shafiee, and H. Bevrani, "Intelligent demand response contribution in frequency control of multi-area power systems," *IEEE Trans. Smart Grid*, vol. 9, no. 2, pp. 1282–1291, Mar. 2018.

[15] N. Soni, S. Doolla, and M. C. Chandorkar, "Improvement of transient response in microgrids using virtual inertia," *IEEE Trans. Power Del.*, vol. 28, no. 3, pp. 1830–1838, Jul. 2013.

[16] Y. Hirase, K. Abe, K. Sugimoto, K. Sakimoto, H. Bevrani, and T. Ise, "A novel control approach for virtual synchronous generators to suppress frequency and voltage fluctuations in microgrids," *Appl. Energy*, vol. 210, pp. 699–710, Jan. 2018.

[17] R. Shi, X. Zhang, C. Hu, H. Xu, J. Gu, and W. Cao, "Self-tuning virtual synchronous generator control for improving frequency stability in autonomous photovoltaic-diesel microgrids," *J. Mod. Power Syst. Clean Energy*, vol. 6, no. 3, pp. 482–494, May 2018.

[18] G. Magdy, G. Shabib, A. A. Elbaset, and Y. Mitani, "A novel coordination scheme of virtual inertia control and digital protection for microgrid dynamic security considering highrenewable energy penetration," *IET Renew, Power Gener.*, vol. 13, no. 3, pp. 462–474, Feb. 2019.

[19] Y. Hu, W. Wei, Y. Peng, and J. Lei, "Fuzzy virtual inertia control for virtual synchronous generator," in *Proc. 35th Chin. Control Conf. (CCC)*, Chengdu, China, 2016, pp. 8523–8527.

[20] K. Mentesidi, R. Garde, M. Agudo, and E. Rikos, "Implementation of a fuzzy logic controller for virtual inertia emulation," in *Proc. IEEE Conf. Smart Elect. Distrib. Syst. Technol.*, Vienna, Austria, Sep. 2015, pp. 606–611.

[21] T. Kerdphol, F. S. Rahman, Y. Mitani, K. Hongesombut, and S. Küfeoğlu, "Virtual inertia control-based model predictive control for microgrid frequency stabilization considering high renewable energy integration," *Sustainability*, vol. 9, no. 5, p. 773, May 2017.

[22] H. Bevrani, *Robust Power System Frequency Control*. New York, NY, USA: Springer, 2009, pp. 15–61.

[23] Y. Han, P. M. Young, A. Jain, and D. Zimmerle, "Robust control for microgrid frequency deviation reduction with attached storage system," *IEEE Trans. Smart Grid*, vol. 6, no. 2, pp. 557–565, Mar. 2015.

[24] M. J. Hossain, H. R. Pota, M. A. Mahmud, and M. Aldeen, "Robust control for power sharing in microgrids with low-inertia wind and PV generators," *IEEE Trans. Sustain. Comput.*, vol. 6, no. 3, pp. 1067–1077, Jul. 2015.

[25] V. P. Singh, S. R. Mohanty, N. Kishor, and P. K. Ray, "Robust H-infinity load frequency control in hybrid distributed generation system," *Int. J. Elect. Power Energy Syst.*, vol. 46, pp. 294–305, Mar. 2013.

[26] H. Bevrani, M. R. Feizi, and S. Ataee, "Robust frequency control in an islanded microgrid: H_∞ and μ-synthesis approaches," *IEEE Trans. Smart Grid*, vol. 7, no. 2, pp. 706–717, Mar. 2016.

[27] A. Fathi, Q. Shafiee, and H. Bevrani, "Robust frequency control of microgrids using an extended virtual synchronous generator," *IEEE Trans. Power Syst.*, vol. 33, no. 6, pp. 6289–6297, Nov. 2018.

[28] X. C. M. Cubillos and L. C. G. de Souza, "Using of H-infinity control method in attitude control system of rigid-flexible satellite," *Math. Problems Eng.*, vol. 2009, pp. 1–9, 2009, Art. no. 173145. doi: 10.1155/2009/173145.

[29] S. Manabe, "Coefficient diagram method as applied to the attitude control of controlled-bias-momentum satellite," *IFAC Proc. Vol.*, vol. 27, no. 13, pp. 327–332, 1994.

[30] *Wikipedia*. Accessed: Sep. 8, 2018. [Online]. Available: https://en.wikipedia.org/wiki/Coefficient_diagram_method

[31] G. Shabib, T. H. Mohamed, and H. Ali, "A real time simulation based new robust load frequency control system," in *Proc. 16th Int. Middle- East Power Syst. Conf. (MEPCON)*, Cairo, Egypt, Dec. 2014, pp. 1–6.

[32] T. H. Mohamed, G. Shabib, and H. Ali, "Distributed load frequency control in an interconnected power system using ecological technique and coefficient diagram method," *Int. J. Elect. Power Energy Syst.*, vol. 82, pp. 496–507, Nov. 2016.

[33] G. Magdy, E. A. Mohamed, G. Shabib, A. A. Elbaset, and Y. Mitani, "SMES based a new PID controller for frequency stability of a real hybrid power system considering high wind power penetration," *IET Renew. Power Gener.*, vol. 12, no. 11, pp. 1304–1313, 2018.

[34] H. Bevrani, B. Francois, and T. Ise, *Microgrid Dynamics and Control*, New York, NY, USA: Wiley, 2017.

[35] S. Manabe, "Importance of coefficient diagram in polynomial method," in *Proc. 42nd IEEE Conf. Decis. Control*, Maui, HI, USA, Dec. 2003, pp. 3489–3494.

[36] A. V. Lipatov and N. I. Sokolov, "On some sufficient conditions for stability and instability of linear continuous stationary systems," *Autom. Remote Control*, vol. 9, no. 39, pp. 1285–1291, 1979.

[37] J. P. Coelho, T. M. Pinho, and J. Boaventura-Cunha, "Controller system design using the coefficient diagram method," *Arabian J. Sci. Eng.*, vol. 41, no. 9, pp. 3663–3681, 2016.

[38] S. Manabe, "Brief tutorial and survey of coefficient diagram method," in *Proc. 4th Asian Control Conf.*, Singapore, Sep. 2002, pp. 25–27.

[39] K. Palaniappan and S. Somasundaram, "Real time implementation of a new CDM-PI control scheme in a conical tank liquid level maintaining system," *Modern Appl. Sci.*, vol. 3, no. 5, pp. 38–45, May 2009.

[40] S. Manabe, "Application of coefficient diagram method to MIMO design in aerospace," in *Proc. 15th Triennial World Congr.*, Barcelona, Spain, 2002, pp. 50–56.

[41] N. Bigdeli and M. Haeri, "CDM-based design and performance evaluation of a robust AQM method for dynamic TCP/AQM networks," *Comput. Commun.*, vol. 32, pp. 213–229, Jan. 2009.

HOSSAM ALI received the B.Sc. and M.Sc. degrees in electrical engineering from the Faculty of Energy Engineering, Aswan University, Aswan, Egypt, in 2012 and 2016, respectively. He is currently pursuing the Ph.D. degree with the Department of Electrical Engineering, Graduate School of Electrical Engineering and Automation, Harbin Institute of Technology, Harbin, China. In 2013, he joined the Department of Electrical Engineering, Faculty of Energy Engineering, Aswan University, first as a Demonstrator and then as an Assistant Lecturer, in 2016. His research interests include power system stability, dynamics, and control, robust control techniques, all applied to power systems, and microgrids.

GABER MAGDY received the B.Sc. and M.Sc. degrees in electrical engineering from the Faculty of Energy Engineering, Aswan University, Aswan, Egypt, in 2011 and 2014, respectively. He is currently pursuing the Ph.D. degree with the Department of Electrical and Electronics Engineering, Graduate School of Engineering, Kyushu Institute of Technology, Kitakyushu, Japan. In 2012, he joined the Department of Electrical Engineering, Faculty of Energy Engineering, Aswan University, first as a Demonstrator and then as an Assistant Lecturer, in 2014. His research interests include power system stability, dynamics, and control, digital control techniques, all applied to power systems, and smart/micro-grid control.

BINBIN LI (S'15–M'17) received the B.S., M.S., and Ph.D. degrees in electrical engineering from the Harbin Institute of Technology, Harbin, China, in 2010, 2012, and 2017, respectively, where he is currently an Associate Professor with the Department of Electrical Engineering. From 2015 to 2016, he was a Visiting Researcher with the Department of Electronic and Electrical Engineering, University of Strathclyde, Glasgow, U.K. His research interests include multilevel converters, high-power electronics, control algorithms, and PWM techniques.

G. SHABIB received the B.Sc. degree in electrical engineering from Al-Azhar University, the M.Sc. degree in electrical engineering from the King Fahad University of Petroleum and Minerals, in 1985, and the Ph.D. degree from Menoufia University, Egypt, in 2001. In 1982, he joined the Electrical Engineering Department, King Fahad University of Petroleum and Minerals, Dhahran, Saudi Arabia, as a Research Assistant. In 1987, he joined the Qassim Royal Institute, Qassim, Saudi Arabia, as a Lecturer. He joined Aswan High Institute of Energy, South Valley University, Aswan, Egypt, in 1999. He joined the Digital Control Laboratory, Tsukuba University, Japan, as a Visiting Professor, from 2006 to 2007. His research interests include power system stability, control, self-tuning control, fuzzy logic techniques, digital control techniques, all as applied to power systems.

ADEL A. ELBASET was born in Nag Hamadi, Egypt, in 1971. He received the B.Sc., M.Sc., and Ph.D. degrees from the Faculty of Engineering, Department of Electrical Engineering, Minya University, Egypt, in 1995, 2000, and 2006, respectively, where he is currently a Staff Member. He was a Visiting Assistant Professor with Kumamoto University, Japan, until 2009. He is currently a Professor with the Department of Electrical Engineering. His research interests include the area of power electronics, power systems, neural networks, fuzzy systems, and renewable energy and optimization.

DIANGUO XU (M'97–SM'12–F'17) received the B.S. degree in control engineering from Harbin Engineering University, Harbin, China, in 1982, and the M.S. and Ph.D. degrees in electrical engineering from the Harbin Institute of Technology (HIT), Harbin, in 1984 and 1989, respectively.

In 1984, he joined the Department of Electrical Engineering, HIT, as an Assistant Professor, where he has been a Professor, since 1994. He was the Dean of the School of Electrical Engineering and Automation, HIT, from 2000 to 2010. He is currently the Vice President of HIT. He has published over 600 technical papers. His research interests include renewable energy generation technology, multi-terminal HVDC system based on VSC, power quality mitigation, speed sensorless vector controlled motor drives, and high performance PMSM servo systems.

Dr. Xu serves as the Chairman of the IEEE Harbin Section. He is an Associate Editor of the IEEE TRANSACTIONS ON INDUSTRIAL ELECTRONICS, the IEEE TRANSACTIONS ON POWER ELECTRONICS, and the IEEE JOURNAL OF EMERGING AND SELECTED TOPICS IN POWER ELECTRONICS.

YASUNORI MITANI (M'87) received the B.Sc., M.Sc., and D.Eng. degrees in electrical engineering from Osaka University, Japan, in 1981, 1983, and 1986, respectively. From 1994 to 1995, he was a Visiting Research Associate with the University of California, Berkeley, USA. He is currently a Professor with the Department of Electrical and Electronic Engineering and the Director of the Industry-Academic Collaboration Division, Kyushu Institute of Technology, Japan. He has authored several books/book chapters, and over 200 journal/conference papers. His research interests include the areas of power system stability, dynamics, and control. He is also the President of the Institute of Electrical Engineers of Japan (IEEJ), Power and Energy Society.